International Journal of Pharmaceutics 591 (2020) 119964

Contents lists available at ScienceDirect

International Journal of Pharmaceutics

journal homepage: www.elsevier.com/locate/ijpharm

The effect of polymer blends on initial release regulation and *in vitro-in vivo* relationship of peptides loaded PLGA-Hydrogel Microspheres

Peifu Xiao [a,b], Pan Qi [b], Jin Chen [b], Zilin Song [b], Yidan Wang [a], Haibing He [b], Xing Tang [b], Puxiu Wang [a,*]

[a] Department of Pharmacy, The First Affiliated Hospital of China Medical University, Shenyang 110001, Liaoning, People's Republic of China
[b] Department of Pharmaceutics, School of Pharmacy, Shenyang Pharmaceutical University, Wenhua Road 103, Shenyang 110016, Liaoning, People's Republic of China

ARTICLE INFO

Keywords:
Peptides microspheres
PLGA blends
Lag time
Initial release regulation
Intrinsic porogen
IVIVR

ABSTRACT

The aim of this study was to resolve the lag time problem for peptides loaded PLGA-Hydrogel Microspheres (PLGA-gel-Ms) by blending low molecular PLGA (Mw. 1 kDa) into PLGA (Mw. 10 kDa) as an intrinsic porogen, and then assess the *in vitro-in vivo* relationship (IVIVR). Here, Goserelin acetate (GOS) was chosen as the model peptides. When compared to additional types of porogen, the intrinsic porogen avoided impurities remaining and protected the bioactivities of the peptides. By adding 10% PLGA (Mw. 1 kDa), the lag time was eliminated both *in vitro* and *in vivo* with a desirable EE (97.04% ± 0.51%). The release mechanisms were found to be: a) initial GOS release mainly controlled by pores diffusion and b) autocatalysis of PLGA (Mw. 1 kDa) which increased the quantity of aqueous pores, as revealed by SEM images. To solve the challenges caused by multiphasic release profiles, for the first time the Segmented phases IVIVR were proposed and developed, and showed improved linear fitting effects and supported the proposed release mechanisms. The application of PLGA blends could provide a new insight into PLGA microsphere initial release rate regulation.

1. Introduction

As a biodegradable and bioabsorbable polymer, which has been approved by the FDA, Poly(lactic-co-glycolic) Acid (PLGA) is widely employed in the microencapsulation of therapeutic peptides or proteins for sustained release (Ye et al., 2010; Li and Jiang, 2018). PLGA microspheres are an effective dosage form for long-acting-release products (LARs) (Shi et al., 2020); and there are a number of commercial LARs drug products of peptides loaded PLGA microspheres on the market such as Lupron Depot®, Sandostatin®, and Decapeptyl® (Wischke and Schwendeman, 2008). These successful products have improved patient compliance and suggest the promising future of peptides loaded PLGA microspheres.

However, due to the high molecular weight, complex structure, and relative instability of peptides and proteins, (Andhariya et al., 2019) the traditional PLGA microspheres preparing methods such as double-emulsion evaporation (W/O/W) (Ye et al., 2010); electrospray (Wang et al., 2019) and spraying drying (Ramazani et al., 2016) faces a series of disadvantages including low drug loading capacity, unoptimistic encapsulation rates and high burst release (Shi et al., 2016). In addition, maintaining the stability of peptides or proteins during the preparation is considered as one of the most significant issues when developing new products (Van der Walle et al., 2009). Hence, developing a suitable preparation method for peptides loaded PLGA microspheres is necessary. It has been reported that a rational concentration of Poloxamer could produce a thermosensitive hydrogel with three-dimensional network structure which could protect peptides or proteins against the hostile environment and retain the high biological activity (Teixeira et al., 2012; Guziewicz et al., 2011; Sellers et al., 2014). Qi et al. demonstrated that by loading Poloxamer hydrogel into PLGA microspheres, not only the biological activity and stability of Goserelin during the preparation process could be protected, but also the drug-loading capacity and the encapsulation efficiency were improved (Qi et al., 2019). Wang et al. prepared an Exenatide loaded PLGA microsphere/thermosensitive hydrogel which reduced the burst release and effectively prolonged delivery (Wang et al., 2017). As the drug release of PLGA-gel-Ms was controlled by both PLGA microsphere and hydrogel structure, the release rate of PLGA-gel-Ms was normally slower than that of PLGA microsphere, resulting in an increased probability of lag time (Wang et al., 2016; Qi et al., 2019).

* Corresponding author.
E-mail address: wpx609612@sina.com (P. Wang).

https://doi.org/10.1016/j.ijpharm.2020.119964
Received 9 August 2020; Received in revised form 22 September 2020; Accepted 6 October 2020
Available online 30 October 2020

Lag time is a plateau phase during which the drug releases from microspheres very slowly, or not at all during the initial period, and is common for injectable long-acting PLGA depots (Schwendeman et al., 2014; Xu et al., 2013; Shang et al., 2018). Typically, the lag time is due to the high fluidity and low ability for water uptake and degradation of PLGA in its glassy state, resulting in less pores for drugs to diffuse throughout the polymer matrix (Klose et al., 2006). Briefly, it appears when the pores and routes between the matrix and the surrounding environment decreased, and leads to large fluctuations in plasma concentration which may influence the therapeutic effect and cause various adverse reactions (Hu et al., 2011; Gu et al., 2018). Eliminating lag time is important to maintain stable plasma concentrations and obtain continuous LARs. There are four commonly used ways to overcome the lag time: 1) creating an acidic pH (Zolnik and Burgess, 2007), 2) adding poorly soluble bases, such as $ZnCO_3$, $Mg(OH)_2$ and $MgCO_3$ (Hirota et al., 2016), 3) blending other water-soluble materials such as PEG 6000 (Buske et al., 2012), and 4) osmotic-transporting (Schwendeman et al., 2014). However, by adding supernumerary agents to form pores, remaining impurities could be introduced, which can cause other problems. In the presence of water, PLGA degradation is an acid-catalyzed reaction which cleaves the ester bonds of the polymer chains and generates acidic oligomers (Versypt et al., 2013). Moreover, it has been shown that the acidic products can in return catalyze the degradation reaction and cause bulk erosion (Gu and Burgess, 2015; Von Burkersroda et al., 2002). Hence, by blending PLGA in low Mw, the degradation of PLGA in high Mw PLGA can be accelerated by accumulated acidic degradation products from PLGA in low Mw (Gu et al., 2015) and thus shortening the lag time.

According to the U.S. FDA guidance, an In Vitro – In Vivo Correlation (IVIVC) is a predictive mathematical model describing the relationship between the *in vitro* and *in vivo* release profiles of a dosage form (Andhariya et al., 2019). There are four main levels of IVIVC categorized by the FDA: Level A, B, C, and multiple Level C. Among them, Level A is a point-to-point correlation mathematical model preferred by the drug review agency, and can provide a guidance for changes in formulations and preparation processes in various stages of development to ensure product quality (Shen et al., 2015). Once a Level A IVIVC of a dosage form has been successfully developed, the *in vitro* release results can be used to predict the true *in vivo* response, so that the pharmacokinetics studies can be minimized and the regulatory burden can be reduced (Shen et al., 2015; Emami, 2006). However, due to their multiphasic release profiles as well as the parenteral complex physiological conditions compared to oral sustained release drug products, there are very few reports on the establishment of IVIVC for PLGA microspheres (Andhariya et al., 2019). An In Vitro – In Vivo Relationship (IVIVR) reflects a relationship that can be described by something other than that of a straight-line (e.g. power, second- or third-order polynomial functions) (U.S-FDA, 2016). Based on FDA guidance document, IVIVR may also be appropriate if they can predict a true drug plasma concentration profile from the *in vitro* data (Nguyen et al., 2017; Mohamed et al., 2020). Therefore, developing an accurate IVIVR for PLGA microsphere is also significant.

In this study, different proportions of PLGA blends were employed to modify the initial release manner of peptides loaded PLGA-gel-Ms. GOS, a synthetic Gonadotrophin-Releasing Hormone analogue (GnRHa) was chosen as the model peptides, as many commercial GnRHa PLGA microspheres (e.g. Lupron Depot®, Suprecur® and Diphereline®) have been successfully developed, while only one marketed product of GOS is an implant (Zoladex®). Subsequently, the GOS PLGA-gel-Ms was evaluated for particle size, Encapsulation Rate (EE), structural morphology, *in vitro* release, and pharmacokinetics investigations. Additionally, the segmented phases IVIVR was proposed and developed to address the challenge of establishing the Level A IVIVC for PLGA microspheres for the first time. These results could provide a guidance in establishing a point-to-point IVIVR for peptides loaded PLGA microspheres. Utilizing PLGA in low Mw as a porogen in the PLGA matrix provides a novel approach for regulating the release manner of PLGA microspheres. Also, overcoming the lag time issue may reduce the limitation of PLGA-gel-Ms in developing LARs of peptides.

2. Materials and methods

2.1. Materials

GOS with purity > 99.2% by high performance liquid chromatography (HPLC) analysis was purchased from Bachem AG Co.Ltd. Carboxyl-terminated PLGA with a 50/50 ration of lactide to glycolide, (Mw. 10 kDa, inherent viscosity = 0.12 dL/g and Mw. 1 kDa, inherent viscosity = 0.025 dL/g) were purchased from Jinan Daigang Biomaterials (Shandong, China). Polyvinyl alcohol (PVA, Mw. 30–70 kDa) was purchased from Kurary Co.Ltd (Japan). Poloxamer 188 (Pluronic® F68) and Poloxamer 407 (Pluronic® F127) were supplied from BASF Co. Ltd (Germany). All other solvents and chemicals were of analytical or chromatographic Grade.

2.2. Preparing process

GOS PLGA-gel-Ms were prepared by a double-emulsion evaporation technique (Qi et al., 2019) according to the formulations listed in Table 1. F1 was the optimized formulation of single PLGA-gel-Ms based on our former research (Qi et al., 2019). F2 – F8 were blend PLGA-gel-Ms which prepared by different rations of PLGA blends. All GOS PLGA-gel-Ms formulations have the same optimized factors except the differences of PLGA. The theoretical drug loading was 14.29%. In order to form the inner hydrogel phase (W_1), 200 mg GOS with 180 mg Poloxamer 188 and 20 mg Poloxamer 407 were mixed in 0.8 mL water and maintained at 4 °C for 10 h. The organic phases (O) were prepared with 1 g PLGA blends dissolved in 4 mL dichloromethane (DCM). In an ice-bath, a primary (W_1/O) emulsion was formed using an Ultra-Turrax TP homogenizer at 12,000 rpm (IKA, Germany) for 2 min. Subsequently, the primary emulsion was injected into 40 mL 1% PVA solution, followed by homogenization for 3 min at the speed of 8000 rpm. Then, the obtained $W_1/O/W_2$ double emulsion was dispersed into 80 mL 3% NaAc solution, magnetically stirred at 20 °C for 2 h for solidification. Finally, the microspheres were washed by purified water three times, lyophilized, and passed through two sieves (74 μm and 37 μm).

2.3. Characterization of GOS PLGA-gel-Ms

2.3.1. Particle size analysis

GOS PLGA-gel-Ms were suspended in purified water before measurement. The particle size and size distribution of PLGA-gel-Ms was

Table 1
Formulation and physical characteristics of GOS PLGA-gel-Ms.

Formulation ID	Proportion of PLGA (10 kDa) to PLGA (1 kDa)	Encapsulation rate (%)	Mean particle size (μm)	Span value
F1	–	92.08 ± 0.43	66.32 ± 2.18	1.430 ± 0.073
F2	1:1	81.58 ± 0.57	65.24 ± 1.82	1.127 ± 0.066
F3	3:1	88.49 ± 0.21	66.41 ± 2.31	1.168 ± 0.095
F4	5:1	92.07 ± 0.38	68.48 ± 2.43	1.128 ± 0.102
F5	9:1	97.04 ± 0.51	63.17 ± 1.94	1.329 ± 0.064
F6	15:1	94.72 ± 0.47	63.66 ± 1.97	1.316 ± 0.070
F7	19:1	97.91 ± 0.36	59.44 ± 1.49	1.592 ± 0.049
F8	24:1	94.16 ± 0.42	60.20 ± 2.01	1.561 ± 0.072

determined (Madani et al., 2018) using a Laser Diffraction Particle Size Analyzer (BT-9300S, Bettersize Co. Ltd., Dandong, China). Every sample was measured in triplicate and calculated for average values. The mean size and particle size distribution was evaluated by mean particle size (D_{v50}) and Span Value. Typically, a narrow size distribution means a Span Value < 5 (Yang et al., 2001), and the smaller span value indicates a narrower size distribution. The span value is calculated by the Eq. (1).

$$\text{Span Value} = (D_{v90} - D_{v10})/D_{v50} \quad (1)$$

where D_{v10}, D_{v50} and D_{v90} are volume size diameters at 10%, 50% and 90% of the cumulative volume, respectively.

2.3.2. Structural morphology

The morphology of GOS PLGA-gel-Ms were determined using a scanning electron microscope (SEM, S-3400, Hitachi High Technologies, Japan) after sputter coating with gold. Atomic force microscopy (AFM, Cypher ES, USA) was performed to investigate the influence of PLGA (Mw.1 kDa) on the microsphere surfaces. The AFM images were generated by utilizing aetrahedral-tipped silicon-etched cantilevers (AC 240Ts-R3, Oxford Instruments) with the resonant frequency from 3100 to 6600 kHz. The Raman volume images were recorded using a Raman microscope (Renishaw in Via reflex, UK) with the characteristic Raman shift data of GOS and PLGA blends (Qi et al., 2019) between 1827 cm^{-1} and 716 cm^{-1}. The Raman volumes of PLGA-gel-Ms in different planes were generated by change the position of incident laser.

2.3.3. Powder X ray diffraction analysis

The powder patterns of GOS, PLGA, Poloxamer, GOS-PLGA-Poloxamer powder mixture (mixed 200 mg GOS, 180 mg Poloxamer 188, 20 mg Poloxamer 407, 500 mg PLGA (Mw. 1 kDa) and 500 mg PLGA (Mw. 10 kDa) and ground in a mortar) and GOS PLGA-gel-Ms lyophilized powder were measured by a D8 Advance X-ray diffractometer (Bruker, Karlsruhe, Germany) from 5 to 60° (2θ) with a 5°/min step rate.

2.3.4. Drug loading (DL) and encapsulation rate (EE)

The quantification of GOS was conducted using a Waters UPLC system (USA) with a UV detector (set wave length at 220 nm). The mobile phase consisted of 0.5% phosphate in acetonitrile and pure water (25:75, v/v) and the flow rate was 0.3 mL/min (Qi et al., 2019). GOS PLGA-gel-Ms (20 mg) were weighed and transferred into a 10 mL volumetric flask. 1 mL acetonitrile and 1 mL glacial acetic acid were added, respectively. Samples were sonicated for 30 s and purified water was used to dilute the solution. Then, the samples were centrifuged at 15,000 rpm for 10 min. The supernatant was determined using the validated UPLC assay as described above. The Drug Loading (DL) and Encapsulation Rate (EE) of GOS PLGA-gel-Ms were determined by Eqs. (2) and (3), respectively.

$$\text{DL} = (\text{the determined mass of GOS in microspheres} \,/\, \text{the mass of GOS microspheres}) \times 100\% \quad (2)$$

$$\text{EE} = (\text{actual DL content} \,/\, \text{theoretical DL content}) \times 100\% \quad (3)$$

All the tests were performed in triplicate.

2.4. In vitro release studies

These studies were carried out in 0.01 M PBS buffer (pH 7.4) to mimic the microenvironment of physiological fluids. Briefly, 40 mg GOS PLGA-gel-Ms were suspended in 2 mL PBS and incubated at 37 ± 0.1 °C in a shaking bath which was vibrating at 100 rpm. At each predetermined time interval, all supernatant was collected after the GOS PLGA-gel-Ms were precipitated by a centrifugation at 3000 rpm for 5 min and then replaced by 2 mL of fresh media. All drug release studies were conducted in triplicate. The amount of GOS released from GOS PLGA-gel-Ms was determined by UPLC as mentioned in 2.3.4.

2.5. Pharmacokinetics study

15 male Sprague–Dawley (SD) rats weighing from 200 to 220 g were randomly divided into three groups of five rats each. Group A was given the single PLGA-gel-Ms (F1) without PLGA (Mw. 1 kDa) at a single dose of 0.9 mg GOS as the control group. Group B was administrated blended PLGA-gel-Ms prepared by the optimized ration of blended PLGA (F5) at a single dose of 0.9 mg GOS as the experimental group. To ensure a good syringeability of microsphere, GOS PLGA-gel-Ms were suspended in 0.5 mL dispersion medium (5% D-mannitol, 0.5% CMC-Na, 0.1% Tween 80 solution) prior to injection. Group C was injected blank saline as the blank group. All SD rats were fasted for 12 h with access to water ad libitum prior to experiments. Groups were injected intramuscularly, and after administration had free access to food and water during the experimental time. This study protocol was executed in compliance with the Animal Experiment Ethics Review of Shenyang Pharmaceutical University. At each predetermined time point, approximately 0.5 mL blood samples were collected in heparinized tubes. The samples were centrifuged (10 min at 5000 rpm) and the supernatant was withdrawn and frozen at −20 °C until analysis.

The GOS content in the plasma was measured using a HPLC-MS system (Applied Biosystems Sciex, Ontario, Canada). According to the literature (Zhang et al., 2014); the mobile phase consisting of A (0.1% formic acid in water) and B (acetonitrile) separated the GOS through gradient elution. The gradient was started at 95% mobile phase B (acetonitrile) and was decreased to 60% over 1.50 min, and then held constant for 1.50 min. At 3.01 min, the column was returned to 95% mobile phase B and was maintained until 6.00 min. The flow rate was 0.4 mL/min.

All obtained pharmacokinetic parameters were calculated by the Drug and Statistics (DAS) software (version 2.0, China) and were expressed as mean ± standard deviation. The AUC was acquired according to the trapezoidal rule and the absorption fraction (f_a) was calculated by the following Eq. (4) (Woo et al., 2001).

$$f_a = (AUC_{0-t}/AUC_{0-\infty}) \times 100\ \% \quad (4)$$

2.6. Development of IVIVR

Due to the long-acting-release characteristic of PLGA microspheres, the tail data is often mixed with the complex absorption phase (Pu et al., 2017). Therefore, using the Nelson-Wagner method to develop the IVIVC (D'Souza et al., 2014) which requires the constant of elimination (k) obtained from the AUC profile may not accurate. Instead, comparing the *in vitro* release with the fractional AUC to develop IVIVR is more rational (Pu et al., 2017).

The total phase IVIVR and segmented phase IVIVR were established through linear fitting the *in vitro* cumulative release and *in vivo* absorption fraction point-to-point. The linear fitting equations were calculated using OriginPro software (version 8.5, OriginLab, USA).

2.7. Statistical data analysis

Statistical analysis was performed using one-way ANOVA by Excel software (version 2016, Microsoft Office, USA), the level of significance was accepted at $p < 0.05$.

3. Results and discussion

3.1. Physicochemical properties of GOS PLGA-gel-Ms

Different GOS PLGA-gel-Ms were prepared by a W/O/W method as described in 2.2. As shown in Table.1, there were no significant differences in particle size distribution between the single PLGA-gel-Ms (F1) and the blended PLGA-gel-Ms (F2 – F8). The similar particle size distribution results could be explained by the viscosity of emulsification system relating to the particle size of the microspheres (Han et al., 2016), whereby Poloxamer hydrogel as the inner phase increased the viscidity of the emulsification system, which offset the influence of adding low molecular weight PLGA. Between F1 to F5, with the increase of PLGA (Mw. 1 kDa) addition, the EE (%) was decreased, which may be due to the PLGA (Mw. 1 kDa) being more hydrophilic compared to PLGA (Mw. 10 kDa) (Park, 1994). It has been reported that the polymer becomes less hydrophobic with decreasing Mw, and at 1100 Da the oligomers become water soluble (Park, 1994; Fredenberg et al., 2011). Part of PLGA (Mw. 1 kDa) may fall out from the PLGA matrix and dissolve into the external aqueous phase during the solidification process,

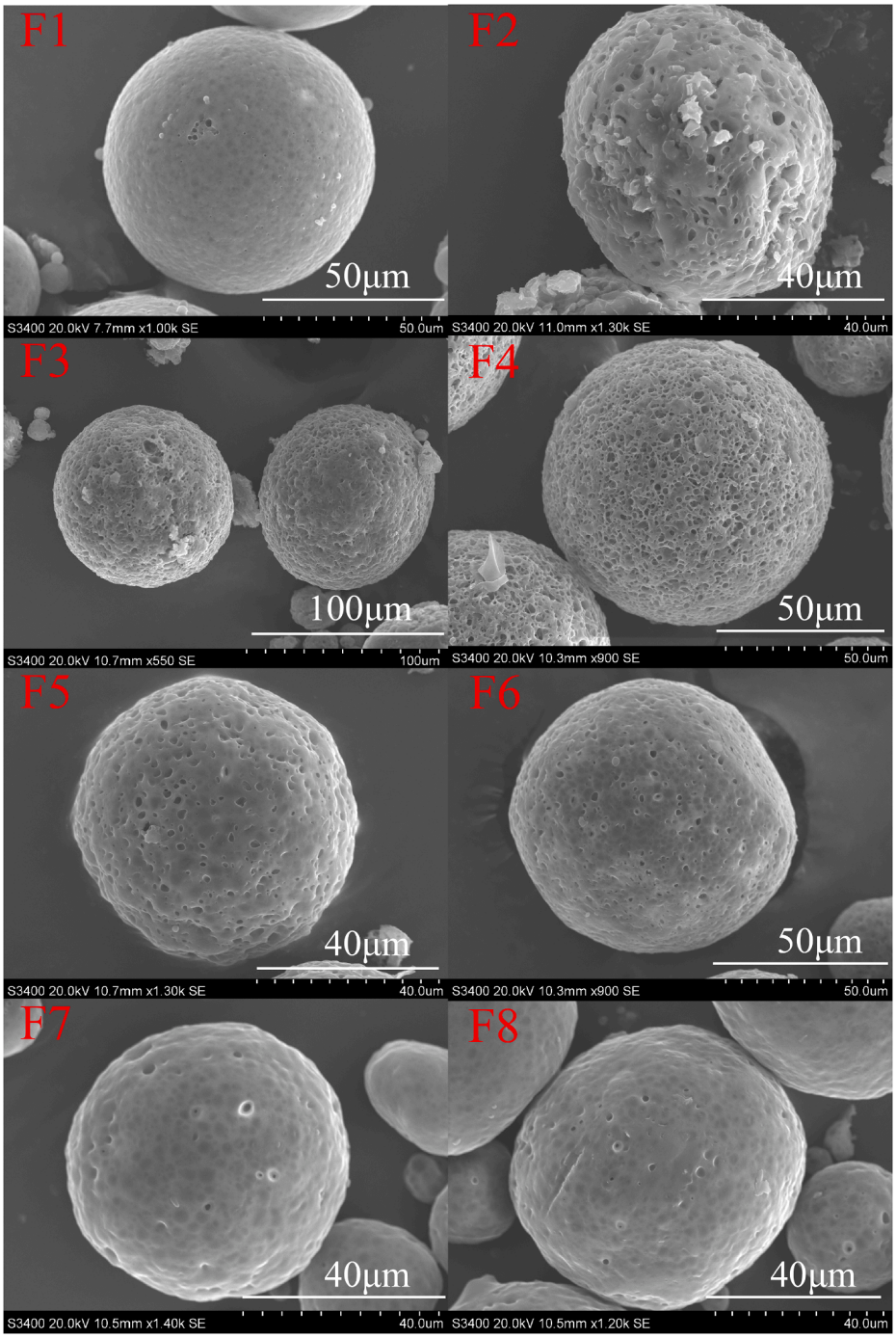

Fig. 1. SEM images of the surface of GOS PLGA-gel-Ms.

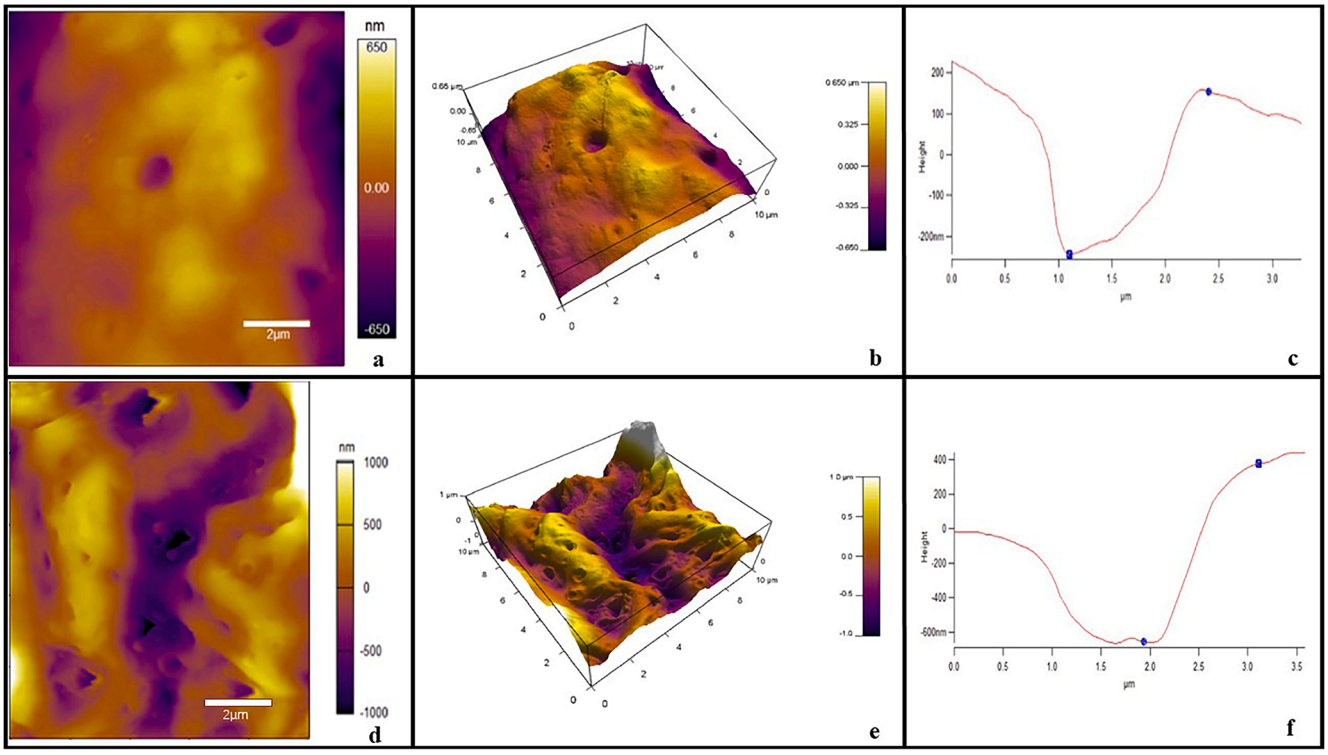

Fig. 2. AFM image of Formulation 1 (graph a, b, c) and Formulation 5 (graph d, e, f). a, b, d, e are the height images of a 10 μm^2 area at the top of a microsphere; c, f are the AFM topography of a surface pore for the microspheres.

causing more aqueous pores to form and the water-soluble GOS leaking outside. This explanation was further confirmed by SEM (Fig. 1) and AFM (Fig. 2) results. From the SEM images, the GOS PLGA-gel-Ms prepared without PLGA (Mw. 1 kDa) showed a smooth surface (F1), however as the PLGA (Mw. 1 kDa) increased, the quantity of pores on the surface also increased. As shown in Fig. 2, compared to single PLGA-gel-Ms (F1), the roughness and the height of pores on the surface of blended PLGA-gel-Ms (F5) increased significantly. The lower weight polymer related to a shorter polymer chain, and improved hydrophilic and softer mechanical properties (Wang et al., 2019). The pores may be formed by PLGA (Mw. 1 kDa), which was hydrated by the diluent during the hardening period, causing water-mediated pore-opening (Desai and Schwendeman, 2013; Reinhold and Schwendeman, 2013). As a result, low weight PLGA easily occupied the channel generated by evaporation of the solvent and formed larger irreversible pores. In conclusion, PLGA (Mw. 1 kDa) as a physical porogen formed additional pores during the preparation period. However, when the ratio of PLGA (Mw. 1 kDa) was less than 10% of PLGA blends, the increase in hydrophilicity was not obvious, resulting in the encapsulation efficiency of F6 - F8 becoming irregular.

The powder X-ray diffraction (PXRD) patterns of individual components and GOS PLGA-gel-Ms are depicted in Fig. 3. The results confirmed

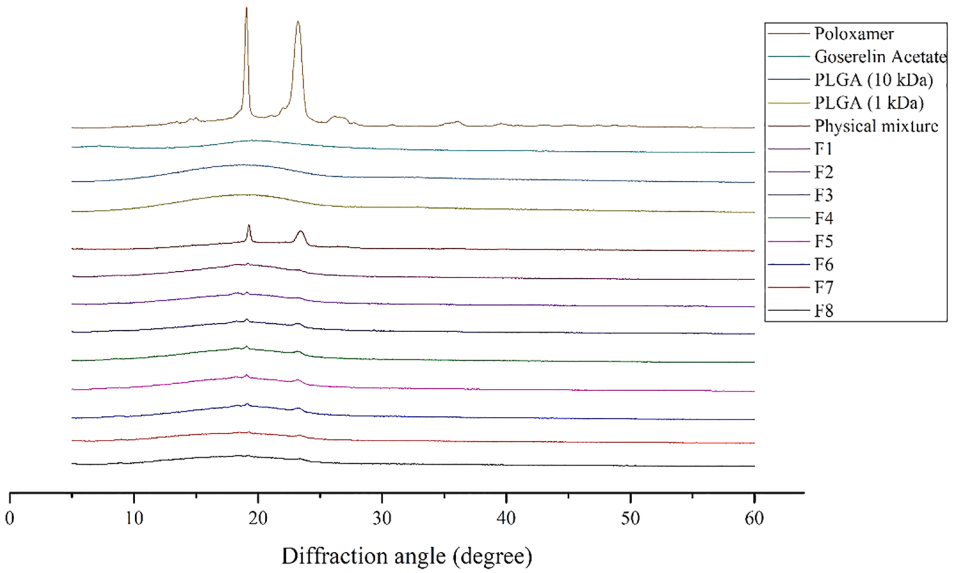

Fig. 3. PXRD curves of single components, Physical Mixture (200 mg GOS, 500 mg PLGA (Mw. 1 kDa), 500 mg PLGA (Mw. 10 kDa), 180 mg Poloxamer 188 and 20 mg Poloxamer 407) and GOS PLGA-gel-Ms (F1-F8).

that GOS exists in an amorphous state and the process of PLGA-gel-Ms preparation didn't change its physical state. The characteristic peak of Poloxamer decreased significantly in PLGA-gel-Ms, suggesting that crystal form of Poloxamer was altered during the lyophilization process, with only minimal Poloxamer remaining in the original crystalline state in GOS PLGA-gel-Ms (Qi et al., 2019). There were no significant differences among F1 - F8, indicating the addition of PLGA (Mw. 1 kDa) did not change the basic crystallinity of the microsphere system.

To identify the structural characteristics and investigate the drug distribution in the GOS PLGA-gel-Ms, stimulated Raman scattering of F5 (PLGA Mw. 10 kDa:1 kDa = 9:1) was performed using Raman shift data between 1827 and 716 cm^{-1}. It depicts GOS distributed within a 80 × 80 × 80 μm^3 volume of a microsphere, which was conducted from −40 μm (bottom of image) to 40 μm (top of image) (Fig. 4). Raman volume images showed a clear core/shell structure, in which GOS (red regions) was wrapped as the inner core while PLGA blends (blue regions) distributed around as the outer shell. It could be observed that some small blue parts appeared in the red regions. This phenomenon revealed that the presence of some GOS and PLGA blends coexisting in the inner core regions. The core/shell structure is not a completely isolated structure, both the core and shell structure blended few substances of another one.

3.2. *In vitro drug release characteristics of GOS PLGA-gel-Ms*

The *in vitro* release studies were carried out in order to investigate how the PLGA (Mw. 1 kDa) could regulate the release manner of GOS PLGA-gel-Ms. As shown in the release profile (Fig. 5), single PLGA-gel-Ms (F1) showed a significant lag phase followed by a secondary release phase. Generally, drug release from PLGA microspheres may be controlled by at least three major mechanisms or their combinations: 1) diffusion through the aqueous pores, 2) diffusion through the polymer matrix and 3) polymer degradation and erosion (Doty et al., 2017). For water-soluble peptides like GOS, water-mediated transport processes should also not be neglected (Fredenberg et al., 2011). For single PLGA-gel-Ms (F1), water penetrated into the microspheres and generated aqueous pores during the initial period (Heya et al., 1994). Subsequently, the inner lyophilized Poloxamer core returned to a viscous hydrogel state after water infiltration (Wang et al., 2017), which effectively slowed down the following water infiltration rate. Simultaneously, PLGA swelled and the pores in the PLGA shell started the process of self-healing (Mazzara et al., 2013). As a result, the water-mediated pores diffusion of F1 was limited. Under the synergistic effect of PLGA shell depot and Poloxamer hydrogel core depot, the cumulative release rate of F1 was 2.56% during the initial 14 days, which is the lag time. PLGA microspheres without hydrogel systems typically have a burst release phase before the lag time, which is caused by drugs on the surface of microspheres which rapidly dissolve in the release medium. According to our former research, PLGA microsphere (F1 without hydrogel system) showed a smooth release without lag phase, and the initial cumulative release in the first 10 h of PLGA-Ms was 3.66% (Qi et al., 2019). However, the initial cumulative release in the first 10 h of F1 was only 0.58%. This could be explained by the majority of the hydrogel being distributed in the inner core, but also the PLGA-gel-Ms having some distribution of hydrogel in the surface pores, which also controlled the initial drug release. After the 14-days lag time, the polymer has been hydrated and lost sufficient mass to start the secondary release, which is controlled by polymer erosion (Cun et al., 2008). This process was confirmed by the morphologies of F1 (Fig. 6A).

Conversely, blended PLGA-gel-Ms (F2-F8) showed a burst release phase followed by secondary release phase, resulting in GOS being released significantly faster than from F1 (Fig. 5). With the addition of PLGA (Mw. 1 kDa) increasing, the cumulative release was also increased, all of which presented an approximative parallel. The initial cumulative release in the first 10 h (Table 2) showed a positive correlation with the addition of PLGA (Mw. 1 kDa) at the proportion range of blended PLGA (Mw. 10 kDa:1 kDa) from 1:1 to 24:1 ($R^2 = 0.998$, fitted by Equation (5)), which could be used for programming a reasonable

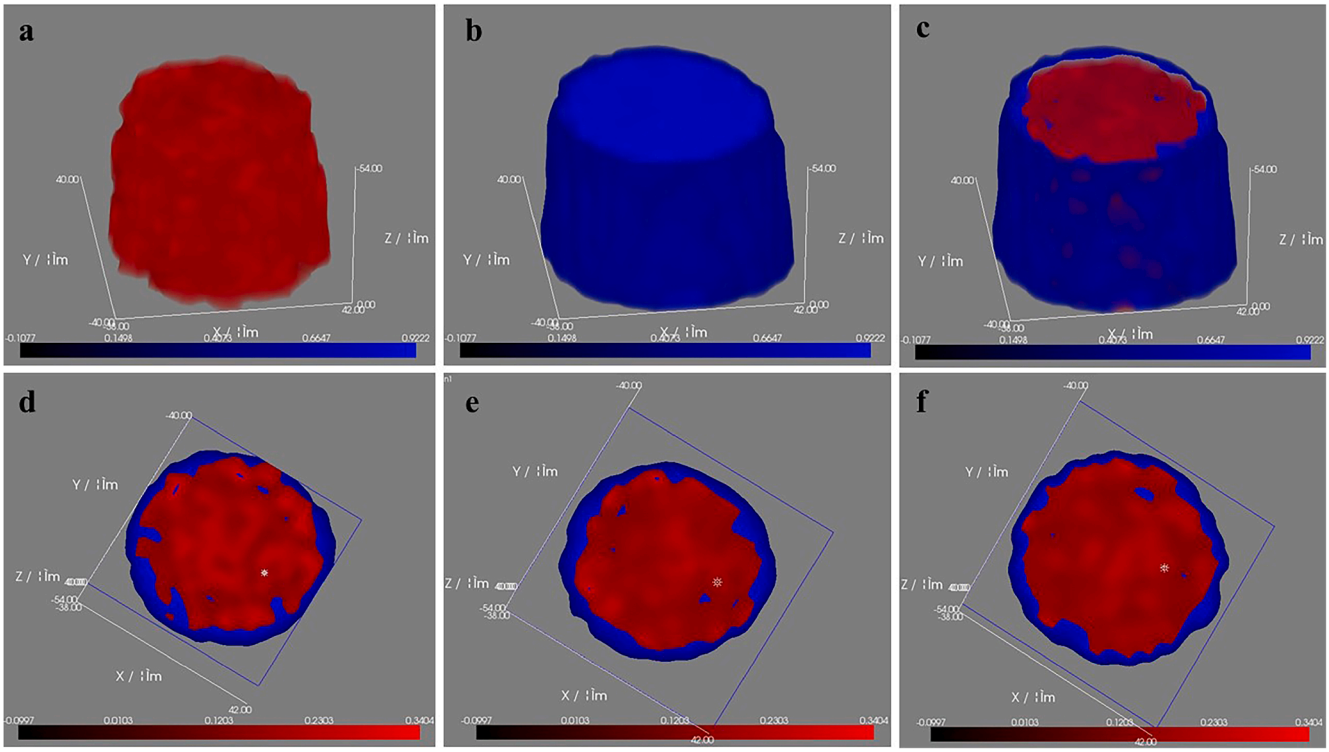

Fig. 4. Raman volume image of Formulation 5. The Red and blue regions in images represent for GOS and PLGA blends, respectively: (a) the image of GOS; (b) the image of PLGA blends (Mw. 10 kDa:1 kDa = 9:1); (c) the image of GOS PLGA-gel-Ms; and (d-f) stimulated Raman scattering of GOS PLGA-gel-Ms at 0, −18 and −36 μm, respectively. (For interpretation of the references to colour in this figure legend, the reader is referred to the web version of this article.)

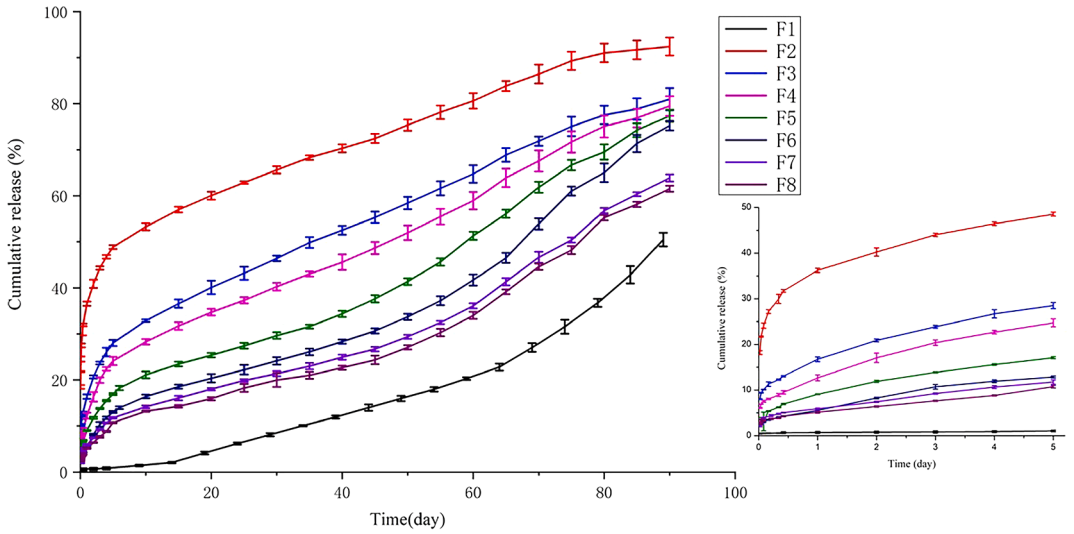

Fig. 5. Effect of PLGA blends on the GOS *in vitro* release from PLGA-gel-Ms: (Formulation 1 is the single PLGA-gel-Ms which was prepared by PLGA (Mw. 10 kDa) alone, Formulation 2 to Formulation 8 corresponds to the blended PLGA-gel-Ms containing PLGA (Mw. 10 kDa) to PLGA (Mw. 1 kDa) at the proportion from 1:1 to 24:1). Microspheres were incubated in PBS 7.4 at 37 °C shaken at 100 rpm to 90 days (n = 3).

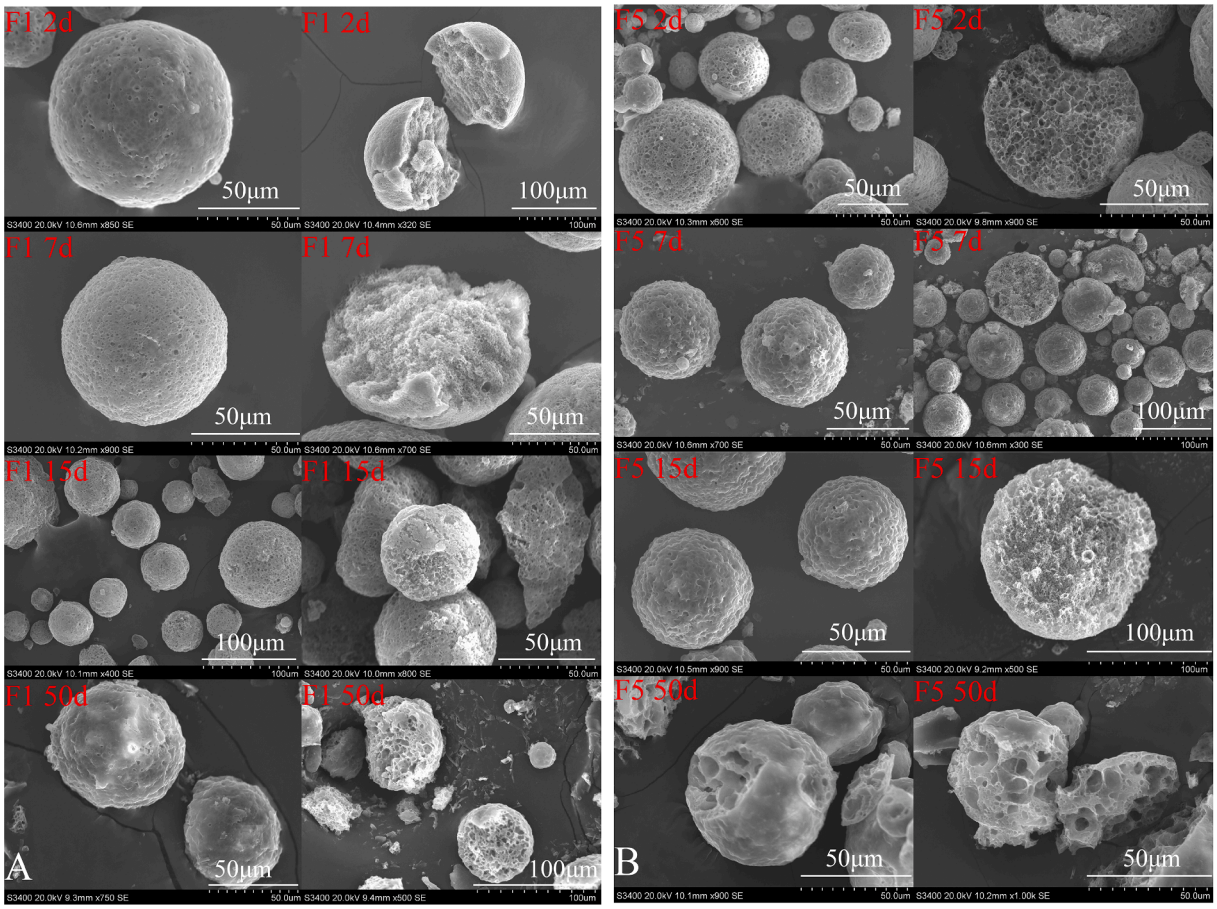

Fig. 6. Surface and inner core SEM images of Formulation 1 (A) and Formulation 5 (B) incubated in PBS 7.4 (at 2, 7, 15, 50 days).

initial release without lag time nor high burst release. As shown in Fig. 5, blended PLGA-gel-Ms have a common release characteristic, where the release rate of the first 5 days is much faster than that of the following days. This result indicates that the release mechanism of blended PLGA-gel-Ms may also be controlled by a combination of two different mechanisms. Typically, the initial release was mainly controlled by pores diffusion and the stable period of drug release was associated with degradation and erosion (Gu et al., 2016). F5 (PLGA Mw. 10 kDa:1 kDa = 9:1), which showed a high Encapsulation Rate (97.04%) and an appropriate *in vitro* release profile (no lag time and the cumulative release in first 10 h was 6.83%), was chosen as the optimized formulation of blended PLGA-gel-Ms to investigate the release mechanism. Here,

Table 2
Cumulative release in first 10 h of different formulations.

Formulation ID	F1	F2	F3	F4	F5	F6	F7	F8
Proportion of PLGA (Mw. 10 kDa: 1 kDa)	–	1:1	3:1	5:1	9:1	15:1	19:1	24:1
Cumulative release (%)	0.58	31.94	12.94	9.23	6.83	4.17	4.96	3.88

$y = 0.313x^{0.7586}$(5).

the first 5 days, 15 days, 50 days were named as the initial period, early stage of the stable period and late stage of stable period respectively. The release mechanisms of F5 in different periods were subsequently investigated in detail.

In the first 5 days, pores diffusion was regarded as the focus of discussion. It has been shown that there is an inversely linear relationship between the rate of drug diffusion and the molecular weight of PLGA (Zhu and Braatz, 2015). In the current research, PLGA (Mw. 1 kDa) accelerated the release rate of GOS by acting as a physical porogen during the preparation process, and acting as a chemical porogen during the initial period. The principle of distinguishing chemical/physical porogen is whether PLGA (Mw. 1 kDa) involved a chemical reaction and generated new substances in this period or not. For blended GOS PLGA-gel-Ms, due to the hydrophilicity of PLGA (Mw. 1 kDa) compared to PLGA (Mw. 10 kDa), more water-mediated pores were generated during the preparation process compared to F1. In the first 10 h, GOS diffused through these aqueous pores, which mainly contributed to the initial burst release. The positive correlation between the degree of burst release and the addition of PLGA (Mw. 1 kDa) was due to the positive correlation between the aqueous pores on the surface and the addition of PLGA (Mw. 1 kDa) in fact. For example, the quantity of pores on the surface were decreased from F2 to F8, and as a result, the initial cumulative release in the first 10 h of F2, F5 and F8 was 31.94%, 6.83% and 3.88% respectively. It should be noted that the hydrogel which distributed in the surface pores also took effect in this period. Without the hydrogel system, the initial cumulative release would further increase and lead to serious burst release. PLGA with a lower molecular weight is more hydrophilic, which facilitates water penetrating into polymers compared with PLGA with higher molecular weights. On the one hand, water penetrated into blended PLGA-gel-Ms easily and generated more aqueous pores. On the other hand, PLGA (Mw. 1 kDa) degraded quickly and its acidic degradation products further accelerated the degradation of the PLGA matrix, leaving more pores in situ. This hypothesis was demonstrated by the increased quantity of aqueous pores on the surface of F5 incubated in the release medium after 2 days (Fig. 6B) compared to the original morphologies (Fig. 1). Our former research has been confirmed that, after the lag time, GOS release in the early stage of the stable release period was mainly by GOS diffusion from the PLGA depot (Qi et al., 2019). Compared to the SEM images of F1, there were more pores on the surface of F5 during the whole initial

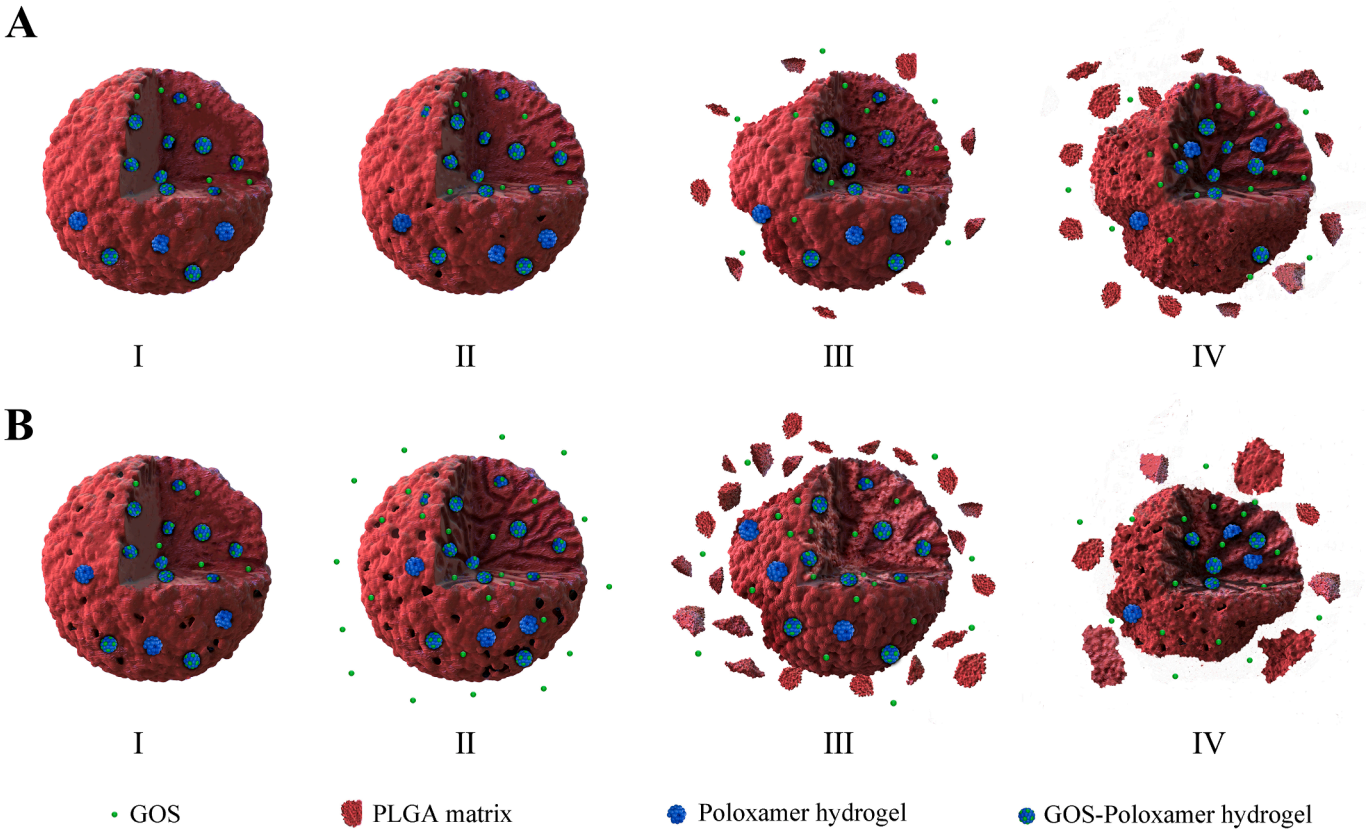

Fig. 7. Schematic illustration of GOS PLGA-gel-Ms and the proposed mechanism for the GOS release from PLGA-gel-Ms during the initial period (Stage I-II) and the stable period (Stage III-IV). Graph A and graph B represent the release process of F1 and F5 respectively. (Stage I (0 day): Different microspheres have different original surface morphology before release. F5 obtained more pores on the surface during the preparation process. Stage II (5 days): GOS diffused through aqueous pores. After water uptake, both F1 and F5 generated aqueous pores. Under the synergistic effect of PLGA and Poloxamer hydrogel, F1 showed a lag time. While with the catalysis of PLGA (Mw. 1 kDa), F5 generated more pores and accelerated the initial release rate significantly. Stage III (15 days): Pores healed and PLGA started erosion. F1 ended the lag time and began its secondary release. F5 ended pores diffusion and turned to matrix erosion. Stage IV (50 days): GOS release controlled by PLGA degradation. F5′s acidic products of PLGA (Mw. 1 kDa) accelerated the degradation reaction of the PLGA matrix).

period (Fig. 6) which accelerated the diffusion rate of GOS from the PLGA depot. As a result, the lag time of F1 was almost eliminated in F5.

After 5 days, the release rate of blended PLGA-gel-Ms slowed down, which may be explained by two aspects of reasons. First, the inner lyophilized Poloxamer core has already been reconstituted as a hydrogel, resulting in blockage of further GOS diffusion from the hydrogel depot (Qi et al., 2019). Besides, the inherent self-healing characteristic of PLGA (Reinhold et al., 2012) also took effect, which could be proved by the SEM morphology of F5 incubated in the release medium (Fig. 6B). The pores were healed and disappeared at the 7th day, and were replaced by hollows on the surface, indicating the water-mediated pores release mechanism during the initial period was replaced by PLGA erosion in the early stage of the stable period. The acidic products of PLGA (Mw. 1 kDa) catalyzed the following PLGA degradation and accelerated GOS release in stable period. As shown in Fig. 6, compared to F1, there were more larger pores both on the surface and in the inner core of F5 at the 50th day. This result suggested that PLGA (Mw. 1 kDa) effectively accelerated bulk erosion of the matrix during the whole stable period, and thus, we believe it would also affect drug release in the terminal period. As a result, though F1 and F5 have the same release and degradation mechanism, the release rate of F5 was much faster than that of F1 in every period due to the presence of PLGA (Mw. 1 kDa). To summarize, the release mechanism of F1 and F5 during the initial period and the stable period was proposed and shown in Fig. 7.

Combining the release profile with the above-mentioned structural morphology, PLGA blends could be utilized for a controllable release characteristic. By altering the amount of PLGA (Mw. 1 kDa) as a physical/chemical porogen, the pores on GOS PLGA Gel-Ms could be regulated, and therefore the initial release rate which was dominated by pores diffusion could be regulated. Compared to porous microspheres prepared by employing additional types of porogen such as $MgCO_3$ or $ZnCO_3$ (Hirota et al., 2016; Zhang et al., 2016), this strategy shows superior performance for its self-accelerating mechanism, which is promising for engineering the release profile.

3.3. Pharmacokinetic evaluation and bioavailability

F 5 (PLGA Mw. 10 kDa:1 kDa = 9:1), which showed a high Encapsulation Rate and an appropriate *in vitro* release profile, was chosen as the optimized formulation to investigate the effect of blended PLGA on GOS absorption *in vivo*. The mean plasma concentration-time curve and pharmacokinetic parameters of single PLGA-gel-Ms (F1) and optimized blended PLGA-gel-Ms (F5) after intramuscular administration to rats are shown in Fig. 8 and Table 3. Compared to the *in vitro* release test, the sampling period *in vivo* was shortened from over 90 days to 49 days, which could be explained by the local acidic pH and biological factors such as enzymes, lipids, organic amines and other endogenous compounds (Fredenberg et al., 2011; Anderson, 2009), which synergistically accelerated the rates of drug release (Zolnik and Burgess, 2008). Particularly, in the terminal period, most PLGA chains were fractured to shorter polymer chains (Versypt et al., 2013), the microspheres were broken and turned into many irregular granules with lower particle size. These granules enlarged the pores, increasing the surface area for drug dissolution and thus accelerated the rate of drug release (Fredenberg et al., 2011).

Table 3
Pharmacokinetics parameters of GOS-gel-Ms and Zoladex® implant (mean ± SD, n = 5).

Parameter	Unit	F1	F5	Zoladex® (Qi et al., 2019)
C_{max}	(μg/L)	218.019 ± 35.147	134.598 ± 3.771	102.905 ± 25.165
T_{max}	(h)	966.2 ± 84.16	806.6 ± 50.35	192.333 ± 165.700
MRT_{0-t}	(h)	897.153 ± 23.182	858.496 ± 57.781	282.358 ± 70.031
AUC_{0-4day}	(μg/L*h)	899.640 ± 456.935	2019.091 ± 921.733	–
AUC_{0-t}	(μg/L*h)	64232.309 ± 15510.585	31721.016 ± 6332.556	6856.016 ± 1966.210
$AUC_{0-\infty}$	(μg/L*h)	201130.677 ± 132639.317	124401.395 ± 105287.685	6865.567 ± 1965.128

The multi-peaks that were observed in the mean plasma concentration-time curve of PLGA-gel-Ms due to the PLGA depot and the inner hydrogel depot respectively (Qi et al., 2019). Compared to the small peak of F1 which occurred at the 12nd day, F5 showed an earlier first small peak at the 2nd day followed by a second small peak at the 9th day (Fig. 8), which indicated the initial GOS release from PLGA depot was accelerated. The two small peaks in the early phase of the mean plasma concentration-time curve indicated two PLGA depots existed in the optimized blended PLGA-gel-Ms (F5). That is, GOS diffused faster in

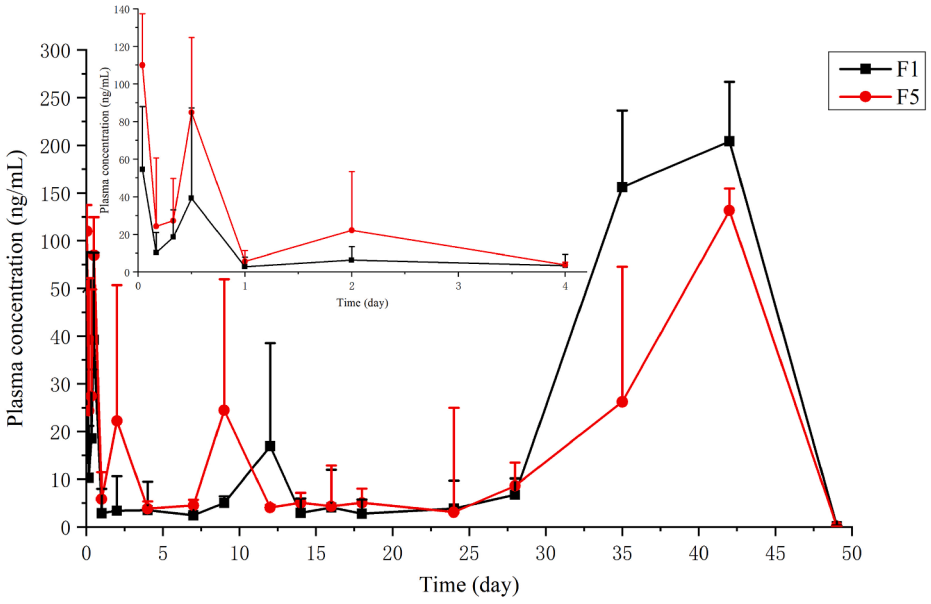

Fig. 8. GOS plasma concentration-time curve after intramuscular injection of single PLGA-gel-Ms (F1) and optimized blended PLGA-gel-Ms (F5) (mean ± standard deviation, n = 5).

the PLGA (Mw.1 kDa) depot due to its faster degradation speed and higher aqueous solubility (Park, 1994), which formed the additional first small peak at the 2nd day. Due to the higher plasma concentration peak from the PLGA (Mw. 1 kDa) depot, the $AUC_{0\text{-}4day}$ of F5 was 2.25-fold (Table 3) greater than that of F1 which provided a better therapeutic effect in initial period. The final large peak of both F1 and F5 appeared simultaneously at the 42nd day, which is formed by GOS release from multi-Poloxamer hydrogels (Yu et al., 2018).

Compared with the Zoladex® implant (Table 3), both F1 and F5 have a significant increase in T_{max} and mean retention time (MRT), suggesting GOS PLGA-gel-Ms could prolong the dosing period of the implant, which is more suitable for a long-acting-release delivery system (Yu et al., 2018). The C_{max} of F5 (134.598 μg/L) was lower than that of F1 (218.019 μg/L) but higher than that of Zoladex® (102.905 μg/L). The $AUC_{0\text{-}t}$ of F5 was 4.63-fold than that of Zoladex®, indicating blended PLGA-gel-Ms could effectively increase the relative bioavailability. Compared to F1, F5 showed an additional small peak of the PLGA depot and a lower larger peak of hydrogel depot. The shorter peak interval and the lower fluctuation in plasma concentration provided F5 with a more stable controlled release manner, which is more suitable for LARs. Besides, F5 solved the lag time problem and reduced the adverse reactions caused by a larger fluctuation of drug concentration in the bloodstream.

The absorption fraction curve of F5 (Fig. 9) and the cumulative release profile showed a similar trend, suggesting PLGA (Mw. 1 kDa) as a porogen could effectively accelerate GOS release both *in vitro* and *in vivo*. The large difference in the *in vitro* cumulative release between F1 and F5 appeared to be reduced for the *in vivo* absorption fraction (e.g. the cumulative release for F5 during the 0-12th day was 22.64% and the value for F1 was only 2.97%, while the absorption fraction for F5 during the 0-12th day was 11.17% and the value of F1 was 2.57%). It has been reported that the high initial release under an *in vitro* environment could be masked to some degree by the *in vivo* absorption at the intramuscular site (Andhariya et al., 2019). Besides, fibrous encapsulation of microspheres through the steric hindrance by the extracellular matrix or the host immune response (Martinez et al., 2010) may lower the *in vivo* burst release (Andhariya et al., 2019). These factors may reduce the difference of GOS plasma concentration between F1 and F5 in the initial period.

By regulating the ratio of PLGA blends, F5 showed a modified release manner without lag time, which could maintain the therapeutic concentrations of GOS during the initial dosing period. The smaller fluctuation in plasma concentration in total time compared to F1 and the higher relative bioavailability compared to Zoladex® indicated F5 has a good application prospect for GOS clinical application.

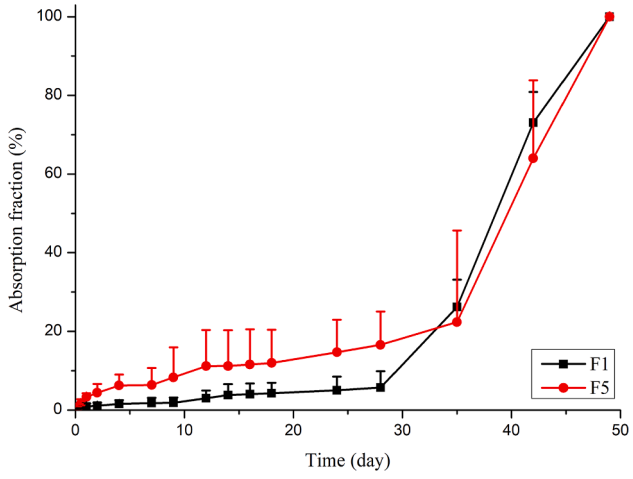

Fig. 9. Absorption fraction in rats receiving microspheres of single PLGA-gel-Ms (F1) and optimized blended PLGA-gel-Ms (F5) (n = 5).

4. Development and discussion of IVIVR

Generally, the *in vitro* evaluation of sustained-release preparations is measured by the cumulative release profile, while the *in vivo* evaluation is reflected by the plasma drug concentration or absorption fraction. Both F1 and F5 showed significant multi-phasic release and *in vitro-in vivo* unsynchronized release characteristics in the current research. F1 under the *in vitro* environment had a nearly 14 days lag time followed by a stable faster secondary release phase. For the *in vivo* release profile, there existed a long low release period between the two peaks formed by PLGA depot and Poloxamer hydrogel depot, so the secondary stable release *in vitro* was replaced by a terminal accelerated release. F5 released fast in the initial period and slowed down in the stable period under the *in vitro* conditions, while a terminal accelerated release was also observed in the absorption fraction curve. As shown in Table 4, the *in vitro - in vivo* relationship coefficient (R^2) of F1 and F5 in total phase was 0.6327 and 0.5263 respectively. The low R^2 indicated the difficulties in establishing a total phase IVIVR of GOS PLGA-gel-Ms. Hence, compared to the conventional IVIVR which linear fits the *in vitro* and *in vivo* release profiles in the total phase, segmenting the correlation according to the time should be more rational. Based on the release mechanism and characteristic, in this study, the total release period was divided into segmented phase I (1–14 days) and segmented phase II (15–49 days) to establish the segmented phases IVIVR respectively.

The *in vitro-in vivo* relationship coefficient (R^2) of both F1 and F5 in segmented phases were increased significantly compared to that the in total phase (Table 4). The improved linear fits and discrimination of the segmented phases IVIVR confirmed the greater applicability for multi-phasic release profiles *in vitro* and *in vivo*.

As shown in Fig. 10, the segmented phases IVIVR equations of F1 and F5 showed similar characteristics in that the slopes were <1 in segmented phase I, while the slopes were >1 in segmented phase II. This result indicated that the *in vitro* release rates were faster than *in vivo* release rates in segmented phase I, while *in vivo* release rates accelerated in segmented phase II. For F1 in segmented phase I, *in vitro* release was slow due to the lag time, while the charge interaction with the extracellular matrix at the intramuscular site may further lower the *in vivo* release rate (Andhariya et al., 2019). For F5, GOS diffused through aqueous pores which were generated by PLGA (Mw. 1 kDa) in the *in vitro* environment, while the high *in vitro* release could be reduced and masked in *in vivo* conditions. In segmented phase II, due to the local acidic pH and biological factors, GOS could diffuse through the pores of broken microspheres resulting in accelerated *in vivo* release rates. An interesting result is that the segmented phases R^2 of F5 were improved compared to F1. This may be ascribed to the difference of release mechanisms between F1 and F5. It has been reported that LARs which mainly controlled by drug diffusion typically have better *in vitro* and *in vivo* correlations than those controlled by PLGA matrix erosion (Pu et al., 2017; Uppoor, 2001).

Through the assessment of segmented phases IVIVR and total phase IVIVR, the current research demonstrated the better applicability of segmented phases IVIVR for PLGA microspheres which have multiphasic release characterizes. Besides, the segmented phases IVIVR in this research suggested the *in vitro* release profile could predict the real absorption *in vivo* to some degree. Further studies could utilize *in vitro* tests to optimize formulations. These results may provide a novel method for establishing a point-to-point IVIVR for peptides loaded PLGA microspheres.

Table 4
In vitro-in vivo relationship coefficient (R^2) of F1 and F5 in total phase and segmented phases.

	F1	F5
Total phase (1–49 d)	0.6327	0.5263
Segmented phase I (1–14 d)	0.9663	0.9951
Segmented phase II (15–49 d)	0.7631	0.8047

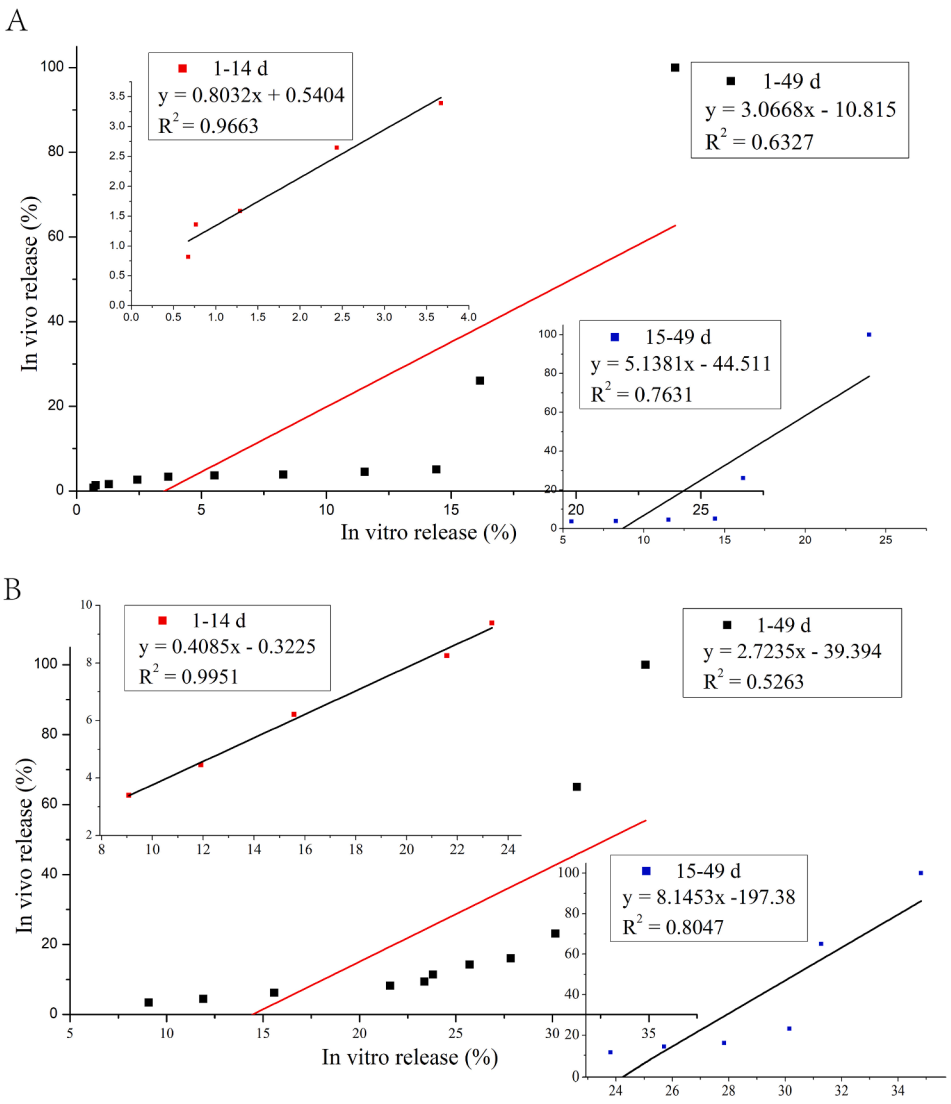

Fig. 10. Point-to-point IVIVR plots of GOS PLGA-gel-Ms. (A) Single PLGA-gel-Ms (F1), R^2 of the total phase (1–49 d) IVIVR was 0.6327, R^2 of the segmented phase I (1–14 d) IVIVR was 0.9663, R^2 of the segmented phase I (15–49 d) IVIVR was 0.7631; (B) Optimized blended PLGA-gel-Ms (F5), R^2 of the total phase (1–49 d) IVIVR was 0.5263, R^2 of the segmented phase I (1–14 d) IVIVR was 0.9951, R^2 of the segmented phase I (15–49 d) IVIVR was 0.8047.

5. Conclusion

Utilizing PLGA-Hydrogel microspheres to protect the biological activity of peptides and obtain LARs shows promise but also faces the challenge of lag time. In this study, PLGA (Mw. 1 kDa) was employed as the intrinsic porogen to regulate the release profile, utilizing the autocatalysis mechanism of PLGA. Combining the *in vitro* cumulative release, Encapsulation Efficiency and structural morphology results of PLGA-gel-Ms, F5 (Mw. 10 kDa:1 kDa = 9:1) was selected as the optimized formulation, in which the problem of lag tine was improved. Two mechanisms: a) GOS diffusion through aqueous pores in the initial period, b) PLGA (Mw. 1 kDa) accelerating the degradation of PLGA matrix were confirmed. In the pharmacokinetic study, the first plasma concentration peak of F5 was advanced by 10 days, which proved the PLGA in low molecular weight also accelerated the initial release *in vivo*. The smaller fluctuation in plasma concentration in total time compared to F1 and the higher relative bioavailability compared to Zoladex® indicated that F5 has a good application prospect for GOS clinical application. Additionally, the autocatalysis mechanism of low molecular weight PLGA is highly promising compared to other alternative supernumerary agents for forming pores. To solve the challenge of establishing Level A IVIVC of PLGA microspheres, the segmented phases IVIVR which have an improved linear fitting effect were established for the first time. The good correlation between *in vitro* and *in vivo* profiles not only provided support for the proposed mechanisms, but also suggested *in vitro* studies could predict real *in vivo* absorption both in this work and in further research. Finally, the proposed solution is expected to provide an alternative for overcoming the lag time problem of peptides loaded PLGA long-acting microspheres.

Funding

This work was supported by the National Natural Science Foundation of China No.81803440.

CRediT authorship contribution statement

Peifu Xiao: Conceptualization, Investigation, Methodology, Writing - original draft, Writing - review & editing. **Pan Qi:** Investigation, Methodology, Writing - review & editing. **Jin Chen:** Methodology, Investigation. **Zilin Song:** Methodology, Investigation. **Yidan Wang:** Methodology, Investigation. **Haibing He:** Formal analysis, Visualization. **Xing Tang:** Conceptualization, Project administration. **Puxiu Wang:** Conceptualization, Visualization, Project administration, Supervision.

Declaration of Competing Interest

The authors declare that they have no known competing financial interests or personal relationships that could have appeared to influence the work reported in this paper.

References

Anderson, J.M., 2009. In vitro and in vivo monocyte, macrophage, foreign body giant cell, and lymphocyte interactions with biomaterials. Biol. Interact. Mater. Surf. 225–244.

Andhariya, J.V., Jog, R., Shen, J., et al., 2019. In vitro-in vivo correlation of parenteral PLGA microspheres: Effect of variable burst release. J. Control. Release. 314, 25–37.

Andhariya, J.V., Jog, R., Shen, J., et al., 2019. Development of Level A in vitro-in vivo correlations for peptide loaded PLGA microspheres. J. Control. Release 308, 1–13.

Buske, J., Koenig, C., Bassarab, S., Lamprecht, A., Muehlau, S., Wagner, K.G., 2012. Influence of PEG in PEG-PLGA microspheres on particle properties and protein release. Eur. J. Pharm. Biopharm. 81 (1), 57–63.

Cun, D., Cui, F., Yang, L., Yang, M., Yu, Y., Yang, R., 2008. Characterization and release mechanism of melittin entrapped poly (lactic acid-co-glycolic acid) microspheres. J. Drug Deliv. Sci. Technol. 18 (4), 267–272.

Desai, K.-G.H., Schwendeman, S.P., 2013. Active self-healing encapsulation of vaccine antigens in PLGA microspheres. J. Control. Release 165 (1), 62–74.

Doty, A.C., Weinstein, D.G., Hirota, K., et al., 2017. Mechanisms of in vivo release of triamcinolone acetonide from PLGA microspheres. J. Control. Release 256, 19–25.

D'Souza, S., Faraj, J.A., Giovagnoli, S., DeLuca, P.P., 2014. In vitro-in vivo correlation from lactide-co-glycolide polymeric dosage forms. Prog. Biomater. 3 (2-4), 131–142.

Emami, J., 2006. In vitro-in vivo correlation: From theory to applications. J. Pharm. Pharm. Sci. 9 (2), 169–189.

Fredenberg, S., Wahlgren, M., Reslow, M., Axelsson, A., 2011. The mechanisms of drug release in poly(lactic-co-glycolic acid)-based drug delivery systems-A review. Int. J. Pharm. 415 (1–2), 34–52.

Fredenberg, S., Jonsson, M., Laakso, T., Wahlgren, M., Reslow, M., Axelsson, A., 2011. Development of mass transport resistance in poly(lactide-co-glycolide) films and particles–a mechanistic study. Int. J. Pharm. 409 (1–2), 194–202.

Gu, B., Burgess, D.J., 2015. Prediction of dexamethasone release from PLGA microspheres prepared with polymer blends using a design of experiment approach. Int. J. Pharm. 495 (1), 393–403.

Gu, B., Wang, Y., Burgess, D.J., 2015. In vitro and in vivo performance of dexamethasone loaded PLGA microspheres prepared using polymer blends. Int. J. Pharm. 496 (2), 534–540.

Gu, B., Sun, X., Papadimitrakopoulos, F., Burgess, D.J., 2016. Seeing is believing, PLGA microsphere degradation revealed in PLGA microsphere/PVA hydrogel composites. J. Control. Release. 228, 170–178.

Gu, B., Papadimitrakopoulos, F., Burgess, D.J., 2018. PLGA microsphere/PVA hydrogel coatings suppress the foreign body reaction for 6 months. J. Control. Release 289, 35–43.

Guziewicz, N., Best, A., Perez-Ramirez, B., Kaplan, D.L., 2011. Lyophilized silk fibroin hydrogels for the sustained local delivery of therapeutic monoclonal antibodies. Biomaterials. 32 (10), 2642–2650.

Han, F.Y., Thurecht, K.J., Whittaker, A.K., Smith, M.T., 2016. Bioerodable PLGA-based microparticles for producing sustained-release drug formulations and strategies for improving drug loading. Front. Pharmacol. 7.

Heya, T.O., Ogawa, Y., Toguchi, H., 1994. In vitro and in vivo evaluation of thyrotrophin releasing hormone release from copoly(DL-lactic/glycolic acid) microspheres. J. Pharm. Sci. 83, 636–640.

Hirota, K., Doty, A.C., Ackermann, R., et al., 2016. Characterizing release mechanisms of leuprolide acetate-loaded PLGA microspheres for IVIVC development I: In vitro evaluation. J. Control. Release 244 (Pt B), 302–313.

Hu, Z., Liu, Y., Yuan, W., Wu, F., Su, J., Jin, T., 2011. Effect of bases with different solubility on the release behavior of risperidone loaded PLGA microspheres. Colloid Surf. B-Biointerfaces. 86 (1), 206–211.

Klose, D., Siepmann, F., Elkharraz, K., Krenzlin, S., Siepmann, J., 2006. How porosity and size affect the drug release mechanisms from PLGA-based microparticles. Int. J. Pharm. 314 (2), 198–206.

Li, X., Jiang, X., 2018. Microfluidics for producing poly (lactic-co-glycolic acid)-based Check for pharmaceutical nanoparticles. Adv. Drug Deliv. Rev. 128, 101–114.

Madani, F., Esnaashari, S.S., Mujokoro, B., Dorkoosh, F., Khosravani, M., Adabi, M., 2018. Investigation of effective parameters on size of paclitaxel loaded PLGA nanoparticles. Adv. Pharm. Bull. 8 (1), 77–84.

Martinez, M.N., Rathbone, M.J., Burgess, D., Huynh, M., 2010. Breakout session summary from AAPS/CRS joint workshop on critical variables in the in vitro and in vivo performance of parenteral sustained release products. J. Control. Release 142 (1), 2–7.

Mazzara, J.M., Balagna, M.A., Thouless, M.D., Schwendeman, S.P., 2013. Healing kinetics of microneedle-formed pores in PLGA films. J. Control. Release 171 (2), 172–177.

Mohamed, L.A., Kamal, N., Elfakhri, K.H., Ibrahim, S., Ashraf, M., Zidan, A.S., 2020. Application of synthetic membranes in establishing bio-predictive IVPT for testosterone transdermal gel. Int. J. Pharm. 586.

Nguyen, M.A., Flanagan, T., Brewster, M., et al., 2017. A survey on IVIVC/IVIVR development in the pharmaceutical industry - past experience and current perspectives. Eur. J. Pharm. Sci. 102, 1–13.

Park, T.G., 1994. Degradation of poly(d, l-lactic acid) microspheres: effect of molecular weight. J. Control. Release. 30, 161–173.

Pu, C., Wang, Q., Zhang, H., et al., 2017. In vitro-in vivo relationship of amorphous insoluble API (progesterone) in PLGA microspheres. Pharm. Res. 34 (12), 2787–2797.

Qi, P., Bu, R., Zhang, H., et al., 2019. Goserelin acetate loaded poloxamer hydrogel in PLGA microspheres: core-shell Di-depot intramuscular sustained release delivery system. Mol. Pharm. 16 (8), 3502–3513.

Ramazani, F., Chen, W., van Nostrum, C.F., et al., 2016. Strategies for encapsulation of small hydrophilic and amphiphilic drugs in PLGA microspheres: state-of-the-art and challenges. Int. J. Pharm. 499 (1–2), 358–367.

Reinhold, S.E., Desai, K.-G.H., Zhang, L., Olsen, K.F., Schwendeman, S.P., 2012. Self-healing microencapsulation of biomacromolecules without organic solvents. Angew. Chem.-Int. Edit. 51 (43), 10800–10803.

Reinhold, S.E., Schwendeman, S.P., 2013. Effect of polymer porosity on aqueous self-healing encapsulation of proteins in PLGA microspheres. Macromol. Biosci. 13 (12), 1700–1710.

Schwendeman, S.P., Shah, R.B., Bailey, B.A., Schwendeman, A.S., 2014. Injectable controlled release depots for large molecules. J. Control. Release 190, 240–253.

Sellers, D.L., Kim, T.H., Mount, C.W., Pun, S.H., Horner, P.J., 2014. Poly(lactic-co-glycolic) acid microspheres encapsulated in Pluronic F-127 prolong hirudin delivery and improve functional recovery from a demyelination lesion. Biomaterials. 35 (31), 8895–8902.

Shang, Q., Zhang, A., Wu, Z., Huang, S., Tian, R., 2018. In vitro evaluation of sustained release of risperidone-loaded microspheres fabricated from different viscosity of PLGA polymers. Polym. Adv. Technol. 29 (1), 384–393.

Shen, J., Choi, S., Qu, W., Wang, Y., Burgess, D.J., 2015. In vitro-in vivo correlation of parenteral risperidone polymeric microspheres. J. Control. Release 218, 2–12.

Shi, Y., Ma, S., Tian, R., et al., 2016. Manufacture, characterization, and release profiles of insulin-loaded mesoporous PLGA microspheres. Mater. Manuf. Process. 31 (8), 1061–1065.

Shi, N.-Q., Zhou, J., Walker, J., et al., 2020. Microencapsulation of luteinizing hormone-releasing hormone agonist in poly (lactic-co-glycolic acid) microspheres by spray-drying. J. Control. Release 321, 756–772.

Teixeira, L.S.M., Bijl, S., Pully, V.V., et al., 2012. Self-attaching and cell-attracting in-situ forming dextran-tyramine conjugates hydrogels for arthroscopic cartilage repair. Biomaterials. 33 (11), 3164–3174.

U.S-FDA, 2016. Modified Release Veterinary Parenteral Dosage Forms: Development, Evaluation, and Establishment of Specifications, in survice, D.o.H.a.H. (Ed.). FDA, USA. pp. 1-18.

Uppoor, V.R., 2001. Regulatory perspectives on in vitro (dissolution)/in vivo (bioavailability) correlations. J. Control. Release 72 (1–3), 127–132.

Van der Walle, C.F., Sharma, G., Kumar, M.N.V.R., 2009. Current approaches to stabilising and analysing proteins during microencapsulation in PLGA. Expert Opin. Drug Deliv. 6 (2), 177–186.

Versypt, A.N.F., Pack, D.W., Braatz, R.D., 2013. Mathematical modeling of drug delivery from autocatalytically degradable PLGA microspheres - a review. J. Control. Release 165 (1), 29–37.

Von Burkersroda, F., Schedl, L., Göpferich, A., 2002. Why degradable polymers undergo surface erosion or bulk erosion. Biomaterials 23, 4221–4231.

Wang, J., Helder, L., Shao, J., Jansen, J.A., Yang, M., Yang, F., 2019. Encapsulation and release of doxycycline from electrospray-generated PLGA microspheres: effect of polymer end groups. Int. J. Pharm. 564, 1–9.

Wang, P., Wang, Q., Ren, T., et al., 2016. Effects of Pluronic F127-PEG multi-gel-core on the release profile and pharmacodynamics of Exenatide loaded in PLGA microspheres. Colloid Surf. B-Biointerfaces 147, 360–367.

Wang, T., Xue, P., Wang, A., et al., 2019. Pore change during degradation of octreotide acetate-loaded PLGA microspheres: the effect of polymer blends. Eur. J. Pharm. Sci. 138, 104990.

Wang, P., Zhuo, X., Chu, W., Tang, X., 2017. Exenatide-loaded microsphere/thermosensitive hydrogel long-acting delivery system with high drug bioactivity. Int. J. Pharm. 528 (1–2), 62–75.

Wischke, C., Schwendeman, S.P., 2008. Principles of encapsulating hydrophobic drugs in PLA/PLGA microparticles. Int. J. Pharm. 364 (2), 298–327.

Woo, B.H., Kostanski, J.W., Gebrekidan, S., Dani, B.A., Thanoo, B.C., DeLuca, P.P., 2001. Preparation, characterization and in vivo evaluation of 120-day poly(D, L-lactide) leuprolide microspheres. J. Control. Release 75 (3), 307–315.

Xu, Q., Chin, S.E., Wang, C.-H., Pack, D.W., 2013. Mechanism of drug release from double-walled PDLLA(PLGA) microspheres. Biomaterials 34 (15), 3902–3911.

Yang, Y.Y., Chung, T.S., Ng, N.P., 2001. Morphology, drug distribution, and in vitro release profiles of biodegradable polymeric microspheres containing protein fabricated by double-emulsion solvent extraction/evaporation method. Biomaterials 22 (3), 231–241.

Ye, M., Kim, S., Park, K., 2010. Issues in long-term protein delivery using biodegradable microparticles. J. Control. Release 146 (2), 241–260.

Yu, M., Yao, Q., Zhang, Y., et al., 2018. Core/shell PLGA microspheres with controllable in vivo release profile via rational core phase design. Artif. Cell. Nanomed. Biotechnol. 46 (Suppl. 1), 1070–1079.

Zhang, S., Han, J., Leng, G., et al., 2014. An LC-MS/MS method for the simultaneous determination of goserelin and testosterone in rat plasma for pharmacokinetic and pharmacodynamic studies. J. Chromatogr. B 965, 183–189.
Zhang, Y., Wischke, C., Mittal, S., Mitra, A., Schwendeman, S.P., 2016. Design of controlled release PLGA microspheres for hydrophobic fenretinide. Mol. Pharm. 13 (8), 2622–2630.
Zhu, X., Braatz, R.D., 2015. A mechanistic model for drug release in PLGA biodegradable stent coatings coupled with polymer degradation and erosion. J. Biomed. Mater. Res. Part A 103 (7), 2269–2279.
Zolnik, B.S., Burgess, D.J., 2007. Effect of acidic pH on PLGA microsphere degradation and release. J. Control. Release. 122 (3), 338–344.
Zolnik, B.S., Burgess, D.J., 2008. Evaluation of in vivo-in vitro release of dexamethasone from PLGA microspheres. J. Control. Release 127 (2), 137–145.